Photoacoustic Monitoring of Adhesive Curing

A. TORRES-FILHO, L. F. PERONDI, and L. C. M. MIRANDA,
Laboratório Associado de Sensores e Materiais, Instituto de Pesquisas Espaciais, Caixa Postal 515, 12201-São José dos Campos, SP, Brazil

Synopsis

The crosslinking reaction of an epoxy-based resin has been monitored by observing the time evolution of the thermal diffusivity of the mixture, using photoacoustic spectroscopy. The results are interpreted in terms of the expected thermal properties of liquids, polymers and solids, and a comparison with the reported viscosity behavior in similar systems is also made. The potential of the technique for following the curing process is discussed.

INTRODUCTION

Photoacoustic (PA) spectroscopy[1] looks directly at the heat generated in a sample, due to nonradiative deexcitation processes, following the absorption of light. In the conventional PA experimental arrangement a sample enclosed in an air-tight cell is exposed to a chopped light beam. As a result of the periodic heating of the sample, the pressure in the chamber oscillates at the chopping frequency and can be detected by a sensitive microphone coupled to the cell. The resulting PA signal depends not only on the amount of heat generated in the sample (i.e, on the optical absorption coefficient and the sample light-into-heat conversion efficiency), but also on how this heat diffuses through the sample. The quantity that measures the rate of heat diffusion in the sample is the thermal diffusivity α, defined by

$$\alpha = k/\rho c \tag{1}$$

where k is the thermal conductivity, ρ is the density, and c is the heat capacity at constant pressure.

The importance of α as a physical quantity to be monitored is due to the fact that, like the optical absorption coefficient, it is unique for each material. This can be appreciated by the tabulated values of α presented by Touloukian et al.[2] for a wide range of materials, such as metals, minerals, foodstuffs, biological specimens, and polymers. In particular, in the case of the polymers, several papers[3-7] have recently been published on the photoacoustic measurement of the thermal diffusivity and conductivity of these materials. These papers employ different versions of the PA technique for evaluating the thermal properties of polymers. In this paper, we discuss the use of the PA technique for monitoring the adhesive curing. The method is basically centered on the monitoring of the thermal diffusivity, as measured by the PA tech-

Journal of Applied Polymer Science, Vol. 35, 103–114 (1988)
 CCC 0021-8995/88/010103-12$04.00

nique, during the cure process. The potential of several techniques that are directly applicable to cure monitoring has been recently reviewed by Fanconi et al.[8] The methods investigated included Fourier transform infrared to monitor crosslinking chemical reactions, dielectric[9] and fluorescence spectroscopies,[10] and ultrasonic attenuation.[11] Needless to say, monitoring techniques and models to correlate monitoring data to improve processing are key aspects to increasing production rates and product quality. The presently proposed PA technique appears to be quite sensitive, requires small amounts of sampling material and is reasonably fast. It also offers an additional advantage over the above-mentioned techniques regarding its versatility. The PA technique may either be used as a spectroscopic technique to monitor the cure chemistry or as a physical monitoring technique. In the former case one looks at the PA infrared spectrum evolution as a function of the curing time. As a physical monitoring technique one uses the PA as a thermal technique to look how the heat diffusion is being affected by the curing process. This second character of the PA technique is the one which we explore in what follows.

EXPERIMENTAL

The experimental arrangement for the PA measurements is schematically shown in Figure 1. It consists of a 250-W halogen lamp whose polychromatic beam is mechanically chopped and focused into the sample which plays the role of a second window closing the PA cell. The disk-shaped sample is supported in a brass ring 450 μm thick with a 5 mm diameter hole. One side of this hole is closed with a 25 μm thick Al foil glued to the brass ring. The rear side of this Al foil, in contact with the outside air and exposed to the rear side light beam illumination, is painted with black ink to enhance the light absorption. The sample supporting brass ring is fixed to the cell body with silicone grease. A commercial electret microphone mounted in one of the cell walls is in contact with the air inside the PA chamber by means of a 1 mm

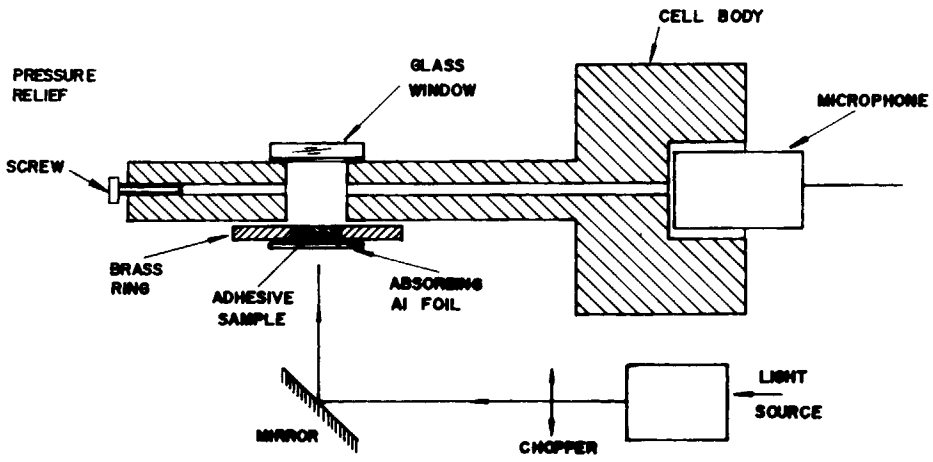

Fig. 1. Schematic arrangement for the PA measurements. The sample fills the hole in the brass ring with 5 mm diameter and 450 μm length.

diameter duct. The signal from the microphone is connected to a lock-in amplifier in which the signal amplitude and phase are both recorded as a function of the modulation frequency.

The above arrangement corresponds to a heat transmission configuration. That is, the heat deposited at the rear-side face of the sample, first diffuses through it before reaching the PA air chamber where it causes the pressure fluctuation detected by the microphone. The thermal wave attenuation[1] in the sample is basically determined by its thermal diffusivity. Thus, by monitoring the PA signal as a function of time one can measure the thermal diffusivity as a function of time. The samples studied were slow-cure epoxy-based adhesives from Ciba-Geigy (Araldite) with different resin-hardner compositions. The chemical composition of this particular epoxy adhesive involves a "bis-epi" type resin, resulting from the reaction of bisphenol A and epichlorhydryn, which can be represented by the structural formula below:

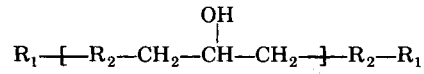

where

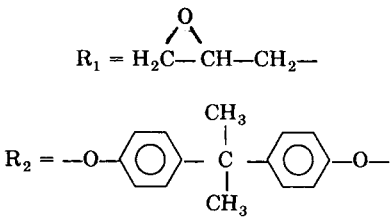

It is cured by a tertiary amine that acts as hardner by inducing a complex ring-opening reaction at the epoxy groups, with the subsequent formation and propagation of a macromolecular anion. Since "bis-epi" resins have epoxy at each end, the amine-induced reaction generates a crosslinked polymeric network. The resin–hardner (R/H) ratios for the sample studied were 2.3 (sample 1), 1.1 (sample 2), and 0.5 (sample 3).

RESULTS AND DISCUSSION

In Figure 2 we show the amplitude of the PA signal at 100 Hz as a function of the normalized curing time τ for the samples studied. The normalized curing time is defined as $\tau = t/t_{\text{final}}$, where t_{final} is the final time of observation where the curing is almost complete. For the samples studied, $t_{\text{final}} = 1396$, 425, and 304 min, for samples 1, 2, and 3, respectively. Figure 2 shows that the PA technique is indeed sensitive to the cure of the adhesive as manifested by the signal amplitude change with the curing time. In particular, we note that the signal corresponding to the larger R–H ratio [Fig. 2(a)] begins the curing process almost immediately. In contrast, samples 2 and 3 begin the curing only after $\tau = 0.13$ (55 min) and $\tau = 0.23$ (69 min), respectively. In fact, sample 2 corresponds to the manufacturer's recommended mixture, and the time lag of roughly 1 h observed for the cure starting agrees with the

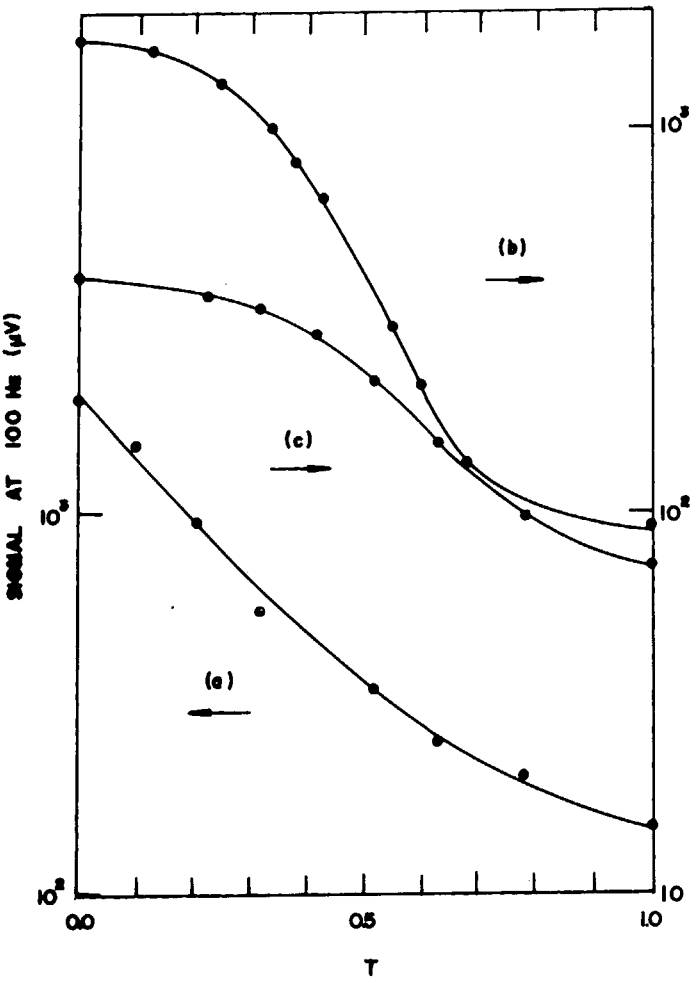

Fig. 2. PA signal amplitude at 100 Hz as a function of the normalized time of cure for the samples studied: (a) sample 1 (R/H = 2.3); (b) sample 2 (R/H = 1.1); (c) sample 3 (R/H = 0.5).

manufacturer's working time suggestion. Two other features should also be noted in Figure 2. First, the signal decreases with decreasing R–H ratio. This agrees with the fact that the pure resin signal is much greater than the pure hardner signal. In fact, at 100 Hz, the ratio of the resin-to-hardner signal was found to be 1.8. Thus, with increasing hardner content in the mixture, one should expect a decrease in the PA signal amplitude as observed in Figure 2. The second point worthwhile noting regards the time scale for the curing process in Figures 2(b) and 2(c). This is given by the slope of the knees in Figures 2(b) and 2(c). Assuming that the knees are described by an exponential law, $\exp(\tau/\tau_0)$, one gets $\tau_0 = 0.15$ (71 min) and $\tau_0 = 0.27$ (82 min) for Figures 2(b) and 2(c), respectively. In other words, increasing the hardner content above 50% there is no significant change in the time scale of the curing process. The main change observed by the increase in the hardner content is in the properties of the final product.

To better understand the PA signal monitoring of the curing process, we have next examined the modulation frequency dependence of the detected signal as a function of the curing time. As is well known,[1] the modulation frequency dependence of the PA signal is the usual way for extracting information about the thermal diffusivity of the material under investigation. This can be seen from the theory of the photothermal effect, as follows.[1,4-7] For the rear-side illumination configuration schematically shown in Figure 3(a), the thermal diffusion model of Rosencwaig and Gersho[12] predicts that the pressure fluctuation p_{th} in the air chamber is

$$p_{th} = \frac{\gamma P_0 I_0 (\alpha_g \alpha_s)^{1/2}}{2\pi l_g T_0 k_s f} \frac{e^{j(\omega t - \pi/2)}}{\mathrm{sh}(l_s \sigma_s)} \tag{2}$$

where γ is the air specific heat ratio, $P_0(T_0)$ is the ambient pressure (temperature), I_0 is the absorbed light intensity, f is the modulation frequency, and l_i, k_i, and α_i are the length, thermal conductivity, and thermal diffusivity of material i, respectively. Here, the subscript i denotes the sample (s) and gas (g), respectively, and $\alpha_i = (1+j)a_i$, $a_i = (\pi f/\alpha_i)^{1/2}$, is the complex thermal diffusion coefficient of material i. In arriving at eq. (2) we have assumed that the sample is optically opaque and that the heat flux into the surrounding air is negligible. The implicit optical opaqueness condition was ensured by the

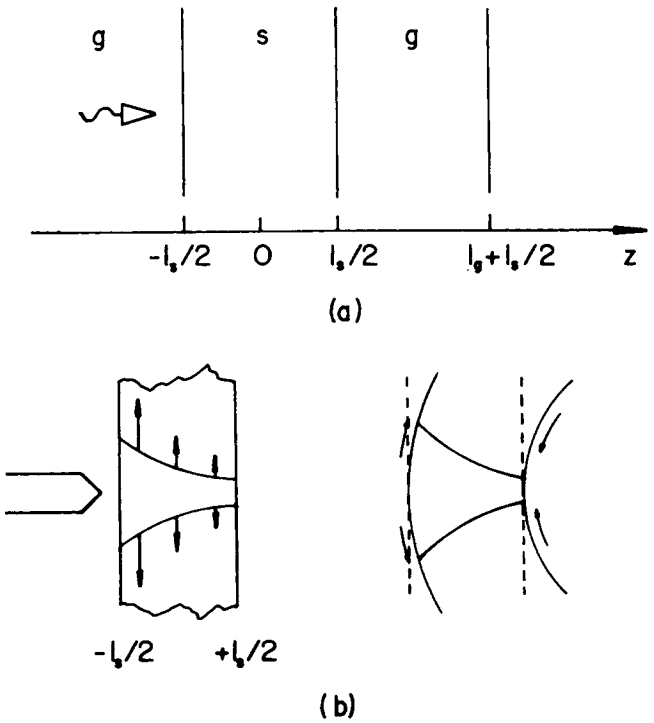

Fig. 3. (a) Schematic geometry for the PA cell; (b) geometry and sources of surface strain for the thermoelastic bending contribution.

thin absorbing Al foil glued to the sample, as described in the previous section. For a thermally thin sample (i.e., $l_s a_s \ll 1$), eq. (2) reduces to

$$p_{\text{th}} \simeq \frac{\gamma P_0 I_0 \alpha_g^{1/2} \alpha_s}{(2\pi)^{3/2} T_0 l_g l_s k_s} \frac{e^{j(\omega t - 3\pi/4)}}{f^{3/2}} \tag{3}$$

In other words, the amplitude of the PA signal decreases as $f^{-1.5}$ as one increases the modulation frequency. In contrast, at high modulation frequencies, such that the sample is thermally thick (i.e., $l_s a_s \gg 1$), one gets

$$p_{\text{th}} \sim \frac{\gamma P_0 I_0 (\alpha_g \alpha_s)^{1/2}}{\pi T_0 l_g k_s} \frac{\exp[-l_s(\pi f/\alpha_s)1/2]}{f} e^{j(\omega t - \pi/2 - l_s a_s)}. \tag{4}$$

Equation (4) means that, for a thermally thick sample, the amplitude of the PA signal decreases exponentially with the modulation frequency as $(1/f)$ $\exp(-af^{1/2})$, where $a = l_s(\pi/\alpha_s)^{1/2}$, whereas its phase ϕ_{th} decreases linearly with $f^{1/2}$, namely, $\phi_{\text{th}} = -\pi/2 - af^{1/2}$. The thermal diffusivity α_s can then be obtained from the high modulation frequency behavior of either the signal amplitude or its phase. In the case of the signal amplitude, α_s is obtained from the experimental data fitting from the coefficient a in the argument of the exponential $(-af^{1/2})$, whereas, when using the signal phase data, α_s is obtained from the phase slope as a function of $f^{1/2}$.

The second contribution to the PA signal comes from the thermoelastic bending of the sample as has been demonstrated by Rousset et al.[13] in both photothermal deflection and conventional PA experiments. This effect is essentially due to the temperature gradient inside the sample along the z-axis and is schematically depicted in Figure 3(b). Due to the existence of this temperature gradient parallel to the z-axis, thermal expansion depends on z. This z dependence of the displacement along the radial direction induces a bending of the plate in the z-direction (drum effect); i.e., the vibrating sample acts as a mechanical piston thereby contributing to the PA signal. The contribution from the sample bending is formally described by the coupled set of thermoelastic equations, similarly to the case of the piezoelectric PA detection.[14] The solution of the thermoelastic equations gives us the sample displacement along the z-direction, from which the thermoelastic contribution p_{el} to the pressure fluctuation in the PA chamber is obtained. One gets [6,13]

$$p_{\text{el}} = \frac{3\alpha_T R^4}{R_c^2} \frac{\gamma P_0 I_0}{l_g k_s} \left[\frac{\text{ch}(l_s\sigma_s) - (l_s\sigma_s/2)\text{sh}(l_s\sigma_s) - 1}{(l_s\sigma_s)^3 \text{sh}(l_s\sigma_s)} \right] e^{j\omega t} \tag{5}$$

where α_T and R are the linear thermal expansion coefficient and radius of the sample and R_c is the radius of the PA chamber. It follows from eq. (5) that for a thermally thin sample ($l_s\sigma_s \ll 1$), the thermoelastic contribution to the PA signal reduces to

$$p_{\text{el}} \simeq \frac{\alpha_T R^4 \gamma P_0 I_0}{8 R_c^2 l_g k_s} e^{j(\omega t + \pi)} \tag{6}$$

In other words, the PA signal becomes independent of the modulation frequency while its phase ϕ_{el} approaches 180°. In contrast, for a thermally thick sample one has

$$P_{el} \simeq \frac{3\alpha_T R^4 \gamma P_0 I_0 \alpha_s}{4\pi R_c^2 l_s^2 l_g k_s f}\left[\left(1-\frac{1}{x}\right)+\frac{1}{x^2}\right]^{1/2} e^{j[\omega t+(\pi/2)+\phi]} \tag{7}$$

where $x = l_s a_s = l_s(\pi f/\alpha_s)^{1/2}$, and

$$\tan\phi = 1/(x-1) \tag{8}$$

Equations (7) and (8) mean that the thermoelastic contribution, at high modulation frequencies such that $x \gg 1$, varies as f^{-1} and its phase ϕ_{el} approaches 90° as

$$\phi_{el} \simeq \pi/2 + \arctan[1/(x-1)] \tag{9}$$

Thus, if the thermoelastic contribution is dominant, the thermal diffusivity can be evaluated from the modulation frequency dependence of either the signal amplitude [eq. (5)] or its phase. Figure 4 shows the theoretically predicted frequency dependence of the PA signal from both the RG model and the thermoelastic bending. The slope corresponding to the RG model at low modulation frequencies is 1.5 [eq. (3)] whereas for high frequencies the signal drops exponentially [eq. (4)]. In Figure 4(b) the signal saturates at low frequencies and behaves as f^{-1} at high frequencies.

In Figure 5 we show the time evolution of the modulation frequency dependence of the PA signal for sample 1 (R/H ≃ 2.3) at t = 0, 169, and 531 min whereas in Figure 6 we present the results for sample 2 (R/H ≃ 1.0) at t = 0, 107, 163, and 425 min. In both cases the low modulation frequency

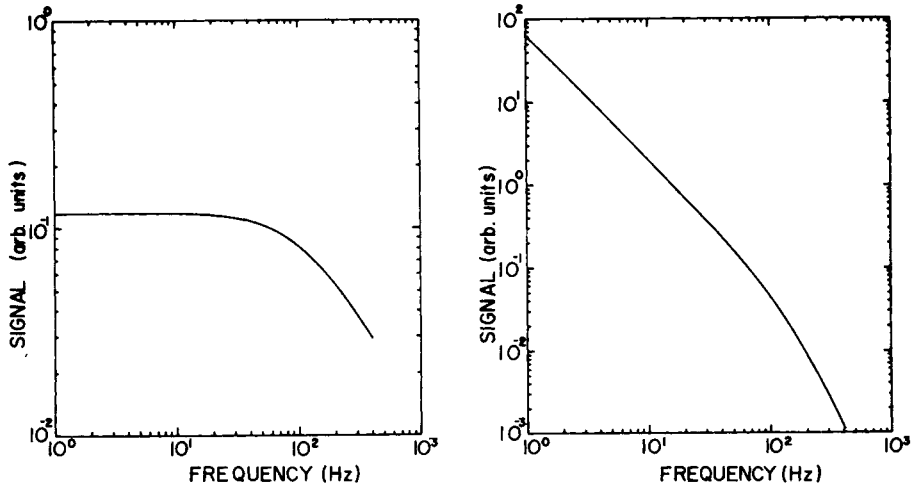

Fig. 4. Modulation frequency dependence of the PA signal predicted by the RG model (a) and the thermoelastic bending (b). The calculation were done using the value of thermal diffusivity of high-density polyethylene (α = 0.0022 cm^2/s) and l_s = 30 μm.

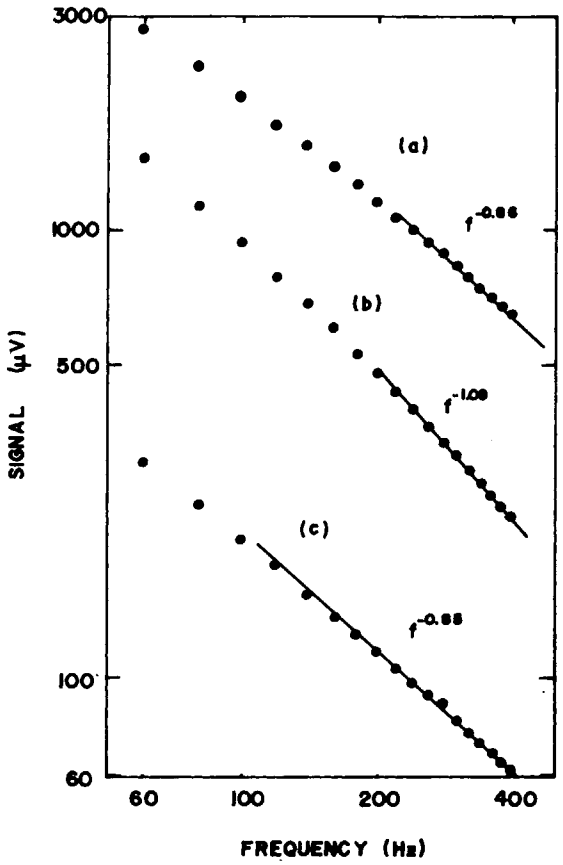

Fig. 5. Time evolution of the modulation frequency dependence of the PA signal for sample 1 (R/H = 2.3) at (a) $t = 0$, (b) $t = 169$ min, and (c) $t = 531$ min.

signal tend to a f^{-x} dependence, with $x \ll 1$, which is close to the Figure 4(b) low-f behavior. At higher frequencies, typically $f > 100$ Hz, the x value tends to increase from an initial value around 0.8, passes through a maximum value higher than 1.0, and returns to $\simeq 1.0$. Comparing these two results and the theoretically predicted signal of Figure 4, we have an indication that thermoelastic bending is the dominant mechanism. We can therefore use eq. (5) to analyze the thermal properties of the adhesive system. According, the measured signal S can be written as

$$S = AF(x) \tag{10}$$

where A is the product of the microphone response and the factor in front of the bracket in eq. (5) and $F(x)$ is the modulus of the bracket in eq. (5). The function $F(x)$, where $x = af^{1/2}$ with $a = l_s(\pi f/\alpha_s)^{1/2}$, gives us the frequency dependence of the observed signal and depends only on the thermal diffusivity. In contrast, the constant A, apart from the geometric factors, light intensity, and so on, depends on the ratio of the thermal expansion coefficient to the thermal conductivity of the sample, namely, $A \sim \alpha_T/k$. We thus have

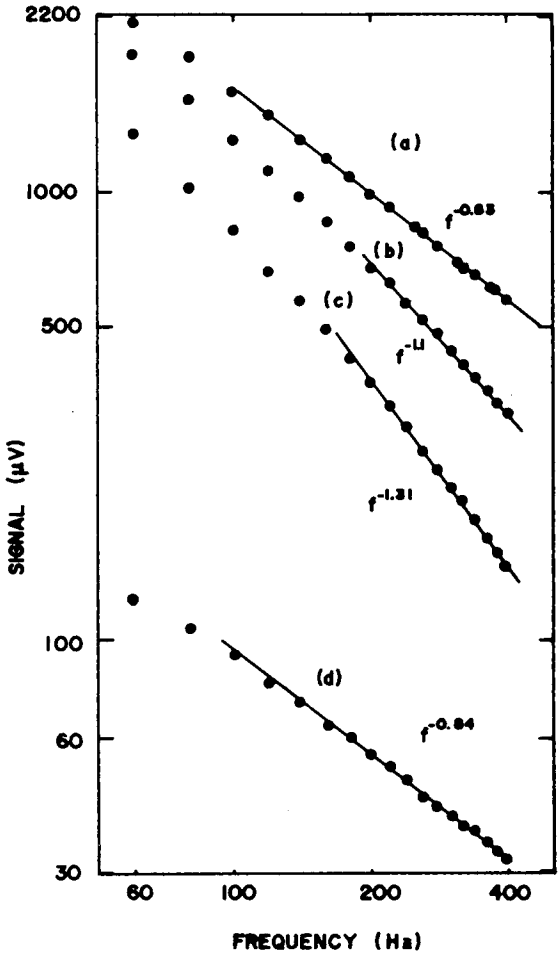

Fig. 6. Time evolution of the modulation frequency dependence of the PA signal for sample 2 (R/H = 1.1) at (a) $t = 0$, (b) $t = 107$ min, (c) $t = 163$ min, and (d) $t = 425$ min.

two adjusting parameters, namely, A and a, to describe the PA monitoring of the cure process. Adjusting these two parameters in the modulation frequency of the PA signal data fitting, one finds the time evolution of the thermal diffusivity α and α_T/k.

In Figure 7 we show the time evolution of the thermal diffusivity normalized to its initial value, namely, $\bar{\alpha} = \alpha/\alpha_0$, for samples 1 and 2. Figure 8 shows the comparison of the time evolution of α and k/α_T for sample 1. As before, the values of k/α_T are normalized to its initial value, $(k/\alpha_T)_0$, and were obtained from $A_0/A = (\alpha_T/k)_0/(\alpha_T/k)$. Figures 7 and 8 show the same overall behavior. After a certain inducing time, there is a sharp decrease in both α and k/α_T which reach a minimum and rise back to a saturation value at the end of the curing process. The data in Figures in 7 and 8 may be explained as follows. As the crosslinking reaction begins to take place, ρ tends to increase. At the same time, one would expect c to increase during the curing process as we move from a liquid to a solid. These two factors suggest

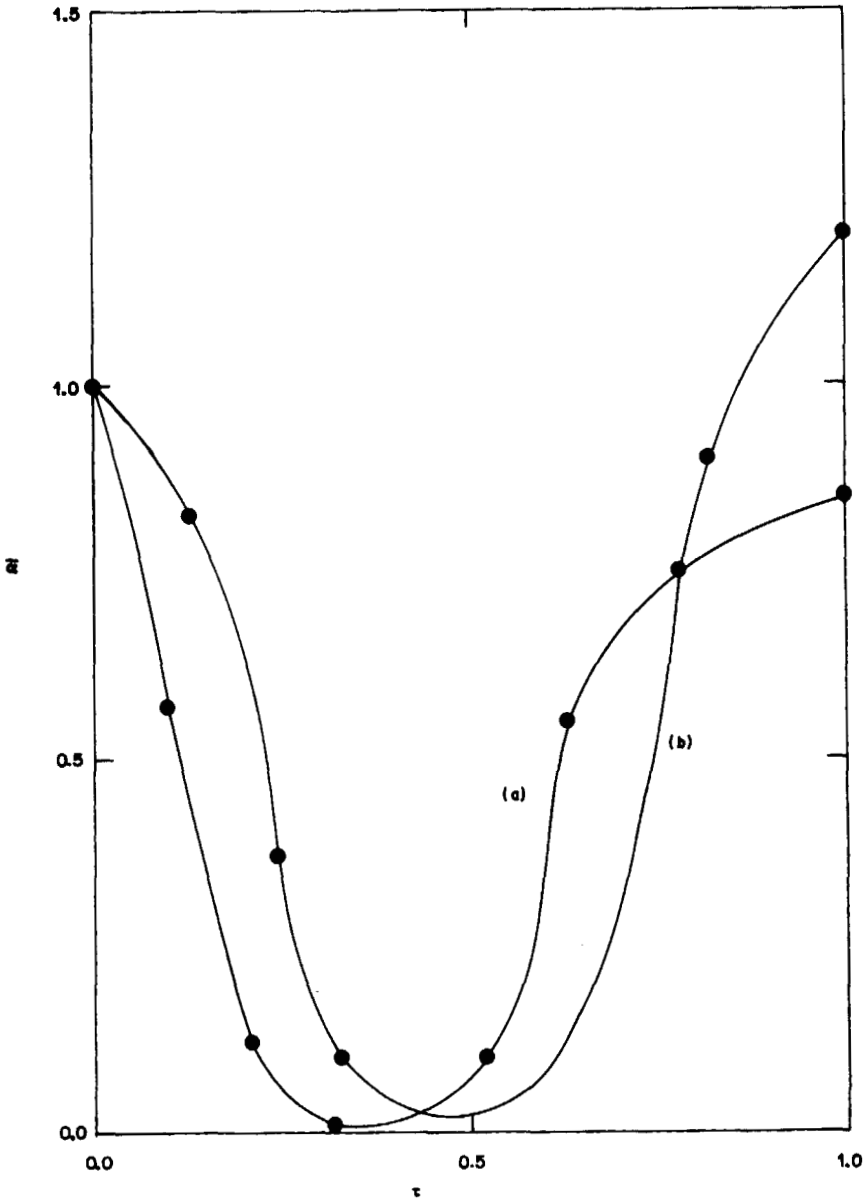

Fig. 7. Curing time evolution of the normalized thermal diffusivity $\bar{\alpha} = \alpha/\alpha_0$ for (a) sample 1 (R/H = 2.3) and (b) sample 2 (R/H = 1.1). The initial values α_0 for each sample was found to be the 0.1024 cm^2/s (sample 1) and 0.0841 cm^2/s (sample 2). The larger value of α of sample 1 with respect to sample 2 is due to the higher resin content in sample 1.

that $\alpha = k/\rho c$ should initially decrease as observed in Figure 7. This is further supported by the decrease in k at the beginning of the curing process as shown in Figure 8(b). In fact, the decrease in k observed in Figure 8(b) may be attributed only to k, since one should expect that α_T decrease monotonically as we move from a viscous fluid (initial mixture) to a solid (small thermal expansion coefficient). After a significant level of hardening has taken place, ρ

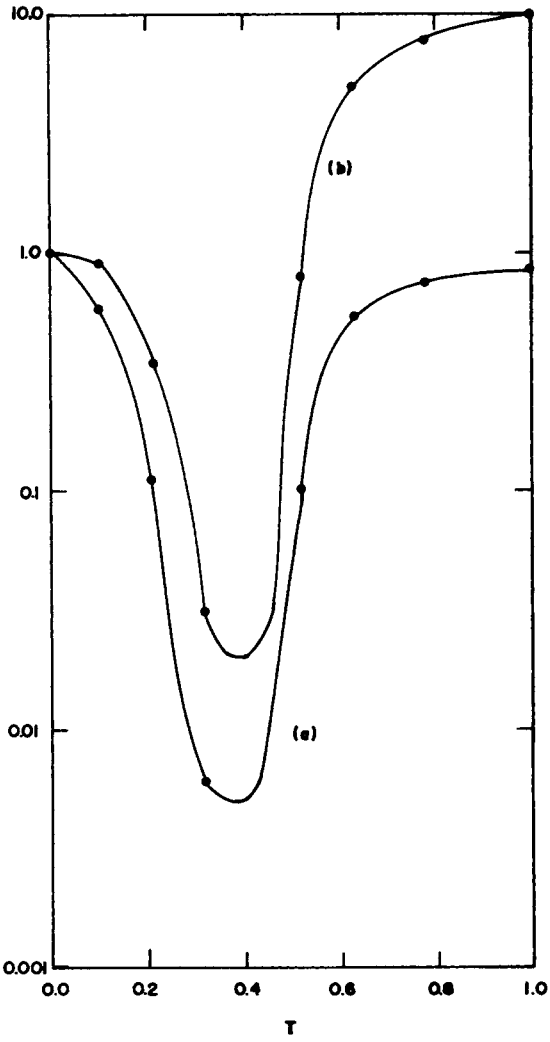

Fig. 8. Curing time evolution of k/α_T normalized to its initial value for sample 1. Since the thermal expansion coefficient α_T is expected to decrease as we move from a viscous fluid to a solid, the initial decrease in this curve is attributed to a decrease of the thermal conductivity.

is practically stabilized and the rise in the thermal diffusivity should be basically due to the rise in the thermal conductivity up to a saturation. The overall shape of the thermal diffusivity curves in Figure 7 shows a very close resemblance to that of the viscosity presented by Fanconi et al.[8] This is consistent with the intuitive expectation that the thermal diffusivity should behave similarly to the viscosity; the higher the thermal diffusivity, the higher the viscosity should be.

Finally, one comment regarding the values of α in the middle of the curing process (region around $\tau = 0.5$ in Fig. 7) should be made. The thermal diffusivity was obtained from the signal data fitting assuming that eq. (5) adequately describes the observed signal. It is therefore, implicitly assumed that during the signal $\times$ modulation frequency data acquisition time (roughly

15 min) the thermal properties do not change considerably. Actually, in the middle of the curing process the physical parameters are rapidly changing, and, therefore, the above assumption is questionable. This is more dramatic in case of sample 2 ($R = 1.1$) for which the signal changes at a faster rate than for sample 1, as a result of the increased hardner content [cf. Fig. 2(b)]. Consequently, in the middle of the curing process, the PA-determined parameters can only be considered as qualitative.

References

1. A. Rosencwaig, *Photoacoustics and Photoacoustic Spectroscopy*, Wiley, New York, 1980.
2. Y. S. Touloukian, R. W. Powell, Y. C. Ho, and M. C. Nicolasu, *Thermal Diffusivity*, Plenum, New York, 1973.
3. P. Korpiun, B. Merté, G. Fritsch, R. Tilgner, and E. Lüscher, *Colloid Polym. Sci.*, **261**, 312 (1983).
4. A. Lachaine and P. Poulet, *Appl. Phys. Lett.*, **45**, 953 (1984).
5. N. F. Leite, N. Cella, H. Vargas, and L. C. M. Miranda, *J. Appl. Phys.*, to appear.
6. L. F. Perondi and L. C. M. Miranda, *J. Appl. Phys.*, to appear.
7. P. Korpiun, R. Tilgner, and D. Schmidt, *J. de Phys.*, **C6**, 43 (1983).
8. B. Fanconi, F. Wang, D. Hunston, and F. Mopsik, *Materials Characterization for Systems Performance and Reliability*, J. W. McCauley and V. Weiss, Eds., Plenum, New York, 1986, p. 275.
9. P. Kranbuchl and T. Hou, *Polym. Eng. Sci.*, **26**, 338 (1986).
10. J. Subocz, *Acta Polym.*, **37**, 266 (1986).
11. D. L. Hunston, in *Review in Quantitative Nondestructive Evaluation*, D. O. Thompson and D. E. Chiminti, Eds., Plenum, New York, 1983, Vol. 2B, p. 1711.
12. A. Rosencwaig and A. Gersho, *J. Appl. Phys.*, **47**, 64 (1976).
13. G. Rousset, F. Lepoutre, and L. Bertrand, *J. Appl. Phys.*, **54**, 2383 (1983).
14. W. Jackson and N. M. Amer, *J. Appl. Phys.*, **51**, 3343 (1980).

Received January 13, 1987
Accepted April 28, 1987